FACETS
a multidisciplinary open access science journal

ARTICLE

Discovery of granulocyte-lineage cells in the skin of the amphibian *Xenopus laevis*

Kelsey Hauser[a†], Milan Popovic[a†], Amulya Yaparla[a], Daphne V. Koubourli[a], Phillip Reeves[b‡], Aashish Batheja[b‡], Rose Webb[c], María J. Forzán[d], and Leon Grayfer[a*]

[a]Department of Biological Sciences, George Washington University, Washington, DC 20052, USA; [b]Thomas Jefferson High School, Alexandria, VA 22312, USA; [c]Pathology Core Laboratory, George Washington University, Washington, DC 20037, USA; [d]Department of Veterinary Biomedical Sciences, College of Veterinary Medicine, Long Island University, Brookville, NY 11548, USA

*leon_grayfer@gwu.edu
[†]KH and MP contributed equally to this work.
[‡]PR and AB are presently affiliated with the University of Virginia, Charlottesville, VA 22904, USA.

Citation: Hauser K, Popovic M, Yaparla A, Koubourli DV, Reeves P, Batheja A, Webb R, Forzán MJ, and Grayfer L. 2020. Discovery of granulocyte-lineage cells in the skin of the amphibian *Xenopus laevis*. FACETS 5: 571–597. doi:10.1139/facets-2020-0010

Handling Editor: David Lesbarrères

Received: February 26, 2020

Accepted: June 17, 2020

Published: July 30, 2020

Note: This paper is part of a Collection titled "Ranavirus research: 10 years of global collaboration".

Published by: Canadian Science Publishing

Abstract

The ranavirus Frog Virus 3 (FV3) and the chytrid fungus *Batrachochytrium dendrobatidis* (*Bd*) are significant contributors to the global amphibian declines and both pathogens target the amphibian skin. We previously showed that tadpoles and adults of the anuran amphibian *Xenopus laevis* express notable levels of granulocyte chemokine genes (*cxcl8a* and *cxcl8b*) within their skin and likely possess skin-resident granulocytes. Presently, we show that tadpole and adult *X. laevis* indeed possess granulocyte-lineage cells within their epidermises that are distinct from their skin mast cells, which are found predominantly in lower dermal layers. These esterase-positive cells responded to (r)CXCL8a and rCXCL8b in a concentration- and CXCR1/CXCR2-dependent manner, possessed polymorphonuclear granulocyte morphology, granulocyte marker surface staining, and exhibited distinct immune gene expression from conventional granulocytes. Our past work indicates that CXCL8b recruits immunosuppressive granulocytes, and here we demonstrated that enriching esterase-positive skin granulocytes with rCXCL8b (but not rCXCL8a) may increase tadpole susceptibility to FV3 and adult frog susceptibility to *Bd*. Furthermore, pharmacological depletion of skin-resident granulocytes increased tadpole susceptibility to FV3. This manuscript provides new insights into the composition and roles of immune cells within the amphibian skin, which is a critical barrier against pathogenic contributors to the amphibian declines.

Key words: granulocytes, skin immunity, innate immunity, amphibian declines, mast cells, IL-8

Introduction

Amphibian species around the globe are facing alarming population declines that also present much broader ecological consequences for the delicate ecosystems they inhabit (Halliday 2008). Recent estimates report close to 40% of known species are experiencing ongoing declines (Scheele et al. 2019) due in large part to emerging infectious agents such as the chytrid fungus *Batrachochytrium dendrobatidis* (*Bd*) and ranaviruses (Stuart et al. 2004; Hayes et al. 2010). Because *Bd* invades keratinized skin, it predominantly affects the adult anuran frogs, whereas anuran tadpole infections are typically nonlethal and are limited to keratinized mouthparts (Berger et al. 1998; Rachowicz and Vredenburg 2004). Conversely, while both tadpole and adult anurans may be infected by ranaviruses like Frog Virus 3 (FV3), tadpoles and metamorphic animals are particularly susceptible and often

succumb to these infections (Green et al. 2002; Duffus and Cunningham 2010). Animal contact is presently thought to be the predominant means of ranavirus transmission (Brunner and Yarber 2018), and we have recently shown that the tadpole skin is an important point of ranaviral entry and a site for viral replication (Wendel et al. 2017).

Amphibian skin mucosa undoubtedly serves as a crucial barrier against, and a major point of contact with, their pathogen-rich environments (Colombo et al. 2015). Moreover, it is indispensable to amphibian water, electrolyte, and gas exchange (Feder and Burggren 1992). Although the integrity of the amphibian skin is intimately linked to the health of these animals, the immune cell composition of amphibian cutaneous tissues remains relatively unexplored. Some frog species possess cells resembling mammalian dendritic and Langerhans cells (Carrillo-Farga et al. 1990; Castell-Rodríguez et al. 2001; Mescher et al. 2007), macrophages, and lymphocytes (Mescher et al. 2007). Granulocytes have also been found in amphibian skin tissues but typically only during times of heightened immune response like infection and injury (reviewed in Grogan et al. 2018).

Granulocyte-lineage mast cells are unique in that they are found within mammalian skin in nonpathological contexts (Galli and Wershil 1996; Baccari et al. 2011). They are also known to populate avian, reptilian, and amphibian skin tissues, although in far fewer numbers (Pelli et al. 2007; Baccari et al. 2011). In more recently diverged vertebrates such as mammals, mast cells are particularly important to immune defenses at primary sites of contact with the environment or pathogens, such as mucosal tissues and skin (Piliponsky et al. 2019). Both their prominent antiviral (Kurane et al. 1984) and antifungal (Nieto-Patlán et al. 2015) capacities are facilitated by numerous compounds stored within their granules. These include heparin and histamine, which are responsible for the characteristic metachromatic granule staining, along with substance P, serotonin, and lectins, which contribute to these cells' ability to destroy pathogens and recruit other immune effectors (Baccari et al. 2011; Sridharan and Shankar 2012). However, much less is known about the precise function of amphibian mast cells in this context and rather, the majority of research has instead focused on mast cells localized in the amphibian tongue and nervous system (Baccari et al. 2011).

We recently characterized several aspects of amphibian granulopoiesis, including roles of the granulocyte chemokine CXCL8 (also known as interleukin-8; IL-8) isoforms in the recruitment of tadpole and adult frog granulocytes (Yaparla et al. 2016; Koubourli et al. 2017, 2018). During those studies, we noted prominent expression of several granulocyte-specific genes, including the *cxcl8a* and *cxcl8b* chemokines as well as the granulocyte growth factor, granulocyte colony-stimulating factor (*gcsf*, also known as *csf3*) and its receptor and granulocyte marker (*gcsfr*, also known as *csf3r*) in the skin of healthy tadpole and adult *Xenopus laevis*. We examined the presence of mast cells as well as a non-mast cell resident granulocyte population within the skin of *X. laevis* tadpoles and adult frogs. Based on our previous findings and given the substantial gaps in the literature, we further sought to address possible roles of these skin immune purveyors in antimicrobial defenses of these animals. The present work contributes to the understanding of the cells that maintain amphibian skin homeostasis and protect these animals from invading pathogens, an imperative endeavor as we look for new conservation approaches.

Materials and methods

Animals

Nieuwkoop and Faber (NF) (Nieuwkoop and Faber 1975) stage 54 outbred tadpoles and approximately 1-year-old, mixed-sex adult *X. laevis* were purchased from Xenopus 1 (Dexter, Michigan, USA). All animals were housed and handled under strict laboratory regulations of the Animal Research Facility at the George Washington University (GWU) and as per the GWU Institutional Animal Care and Use Committee regulations (Approval number 15-024).

Cell culture maintenance

All cell cultures were established in amphibian serum-free medium supplemented with 10% fetal bovine serum, 0.25% *X. laevis* serum, 10 µg/mL gentamicin (Thermo Fisher Scientific, Waltham, Massachusetts, USA), 100 U/mL penicillin, and 100 µg/mL streptomycin (Gibco, Thermo Fisher Scientific). Amphibian phosphate buffered saline (A-PBS) has been previously described (Koubourli et al. 2017).

Production of recombinant frog cytokines and chemokines

The production of recombinant granulocyte colony-stimulating factor (rG-CSF), rCXCL8a, rCXCL8b, and the recombinant control (r-ctrl) was described by Koubourli et al. (2018) and Yaparla et al. (2018). In brief, the recombinant cytokines were produced by generating expression constructs containing the signal peptide-cleaved representations of the respective cytokine cDNAs in the pMIB/V5 His A insect expression vector (Invitrogen, Carlsbad, California, USA) backbone and transfecting these into Sf9 insect cells (Cellfectin II, Invitrogen). Positive transfectants were scaled up to 500 mL cultures, grown for 5 d, and the recombinant proteins isolated from the supernatants of these cultures using Ni-NTA agarose (Qiagen, Hilden, Germany) columns as described by Koubourli et al. (2018) and Yaparla et al. (2018). The r-ctrl was produced by transfecting Sf9 cells with an empty pMIB/V5 His A insect expression vector (Invitrogen) and processing the supernatants from the resulting transfected cultures using the same methodology as described for the above cytokines.

Anti-*X. laevis* granulocyte colony-stimulating factor receptor (G-CSFR) polyclonal antibody

The production of the polyclonal rabbit IgG against the recombinant *X. laevis* G-CSFR was described by Koubourli et al. (2018). In brief, a recombinant *X. laevis* G-CSFR (1 mg total) was generated and submitted for rabbit immunization protocols (ProSci Inc., Fort Collins, Colorado, USA). The resulting rabbit immune serum was assessed by western blot against the rG-CSFR and applied to a HiTrap Protein A HP column (GE HealthCare Life Sciences, Marlborough, Massachusetts, USA) to isolate the IgG fraction. A Sulfo-Link Protein Kit (Thermo Fisher Scientific) was then used according to the manufacturer's instructions to purify the IgG fraction that cross-reacted with the rG-CSFR.

Granulocyte enrichment, isolation, and pharmacological depletion in *X. laevis*

Tadpole and adult frog granulocytes were generated as previously described by Koubourli et al. (2017). Briefly, rG-CSF in A-PBS (10 µL final volume) was pipetted onto parafilm, taken up with finely pulled glass needles and injected into the peritonea of tadpoles (1 µg/tadpole) and adult frogs (5 µg/frog). Twenty-four hours following injection, total peritoneal leukocytes were lavaged with 2×25 µL volumes of A-PBS and subsequently enumerated via a hemocytometer using a 1:1 dilution of cell suspension to 0.4% Trypan Blue (Sigma-Aldrich, St. Louis, Missouri, USA) to account for dead and dying cells.

To enrich the frog skin granulocytes, tadpoles and adult frogs were respectively injected subcutaneously with 0.5 or 2.5 µg of rCXCL8a, rCXCL8b or equal volumes of r-ctrl in 5 µL of A-PBS using finely pulled glass needles. Skins were collected for further analysis 24 h postinjection.

The tadpole and adult skin granulocyte numbers were pharmacologically reduced by subcutaneously injecting animals with 50 mg/kg of reparixin (CXCR1/2 inhibitor; MedChemExpress, Monmouth Junction, New Jersey, USA) in 5 µL of A-PBS using finely pulled glass needles and a 6 h time of treatment, established during preliminary experiments.

Frog Virus 3 stocks and infections

Frog Virus 3 (FV3; wild type, ATCC VR-567) production was previously described by Morales et al. (2010). In brief, baby hamster kidney (BHK-21) cells were infected with FV3 (multiplicity of infection; MOI: 0.1), grown at 30 °C and 5% CO_2 for 5 d. The FV3-containing supernatants were collected over 30% sucrose by ultracentrifugation, resuspended in saline and the viral titers were determined by plaque assay over BHK-21 cells.

Tadpole (stage NF 54–56) skin granulocytes were manipulated as described above, at which time (24 h post-CXCL8a/b injection or 6 h postreparixin injection) the animals were challenged for 1 h in a 100 mL water bath containing 1×10^6 plaque forming units (PFU) (i.e., 1×10^4 PFU FV3/mL water). Animals were then washed in FV3-free water and housed for an additional 24 h, euthanized by tricaine mesylate (TMS) overdose and the dorsal skin tissues collected for histology or RNA/DNA isolation, as described below.

Batrachochytrium dendrobatidis stocks and infections

Batrachochytrium dendrobatidis (*Bd* isolate JEL 197; a kind gift from Dr. Louise Rollins-Smith) was grown in 1% tryptone broth or on 1% tryptone agar plates (Difco Laboratories, Detroit, Michigan, USA; Flechas et al. 2019), supplemented with 100 U/mL penicillin and 100 µg/mL streptomycin (Gibco) at 21 °C.

For *Bd* infection studies, confluent *Bd*-tryptone plates were flooded with water to release zoospores, which were enumerated and used for water bath infections. Adult frog (approximately 1 year old) skin granulocytes were manipulated as described above, and the animals were challenged with 10^7 zoospores of *Bd* in 100 mL of water. After 3 h, an additional 400 mL of water was added to frog tanks and the animals were housed for an additional 7 d before being euthanized and their skins processed for histology or RNA/DNA isolation, as described below.

Acquisition of *X. laevis* skin tissue for chemotaxis assay and gene expression

Tadpole and adult *X. laevis* were euthanized by TMS overdose and 5 mm^2 sections were removed from their dorsal skin surfaces using sterilized forceps and scissors for chemotaxis and gene expression assays. Dorsal skin was removed in the same manner for histology. Skin samples were used immediately after transection for chemotaxis assays, placed in Trizol reagent (Invitrogen) for gene expression analyses, or placed in 10% neutral buffered formalin (VWR, Radnor, Pennsylvania, USA) for histology fixation.

Chemotaxis assays

All chemotaxis assays were performed using blind well Boyden chambers (Neuro Probe, Gaithersburg, Maryland, USA). The bottom wells were loaded with culture medium alone or medium containing 10^2–10^{-8} ng/mL of rCXCL8a or rCXCL8b in 100 µL of medium. The wells were then overlaid with 13 mm chemotaxis filters (5 µm pore size; Neuro Probe) and tadpole ($N = 3$–6 per chemokine concentration) or adult frog ($N = 3$–6 per chemokine concentration) skin sections (obtained as detailed above) were oriented in the top wells such that the dermal layer was closest to the filter in 100 µL medium. The tadpole and adult frog skin granulocyte chemotaxis towards the most chemo-attractive concentrations of rCXCL8a and rCXCL8b was confirmed three times, independently.

After 3 h of incubation at 27 °C with 5% CO_2, the top layers were aspirated and the topsides of the filters were wiped with cotton swabs. The bottom faces of the filters were then stained with Giemsa

(Gibco, Thermo Fisher Scientific) and migrating cells quantified by counting 10 random fields of view per filter (40× objective).

The chemokinesis (gradient-independent cell migration) experiments were performed by loading 10^{-4} ng/mL of rCXCL8a or rCXCL8b (the most chemo-attractive concentration) to both the bottom and the top wells of the chemotaxis chambers, in conjunction with tadpole or adult frog skin sections in medium in the top wells. After 3 h of incubation, the migrating cells were enumerated as above.

The CXCR1 and CXCR2 inhibition studies were carried out using reparixin (MedChemExpress). The optimal dose (10^{-4} ng/mL) of rCXCL8a or rCXCL8b was loaded to bottom chemotaxis chambers and tadpole or adult skin sections in conjunction with reparixin (1 nM final) in the upper chambers. After 3 h of incubation, the migrating cells were enumerated as above.

For all gene expression and pathogen exposure studies, 10^{-4} ng/mL of rCXCL8a or rCXCL8b was used to chemo-attract cells out of the tadpole or adult skin sections ($N = 5–6$ per chemokine, 5 mm^2). The cells were collected from bottom wells of the Boyden chambers and enumerated by hemocytometer counts using a 1:1 dilution of cell suspension in A-PBS to 0.4% Trypan Blue (Sigma-Aldrich, St. Louis, Missouri, USA) to account for dead cells.

For anti-G-CSFR and esterase activity analyses of the tadpole and adult skin granulocytes, cells isolated from six individual tadpole or adult skins (from six bottom chemotaxis chambers) were combined and cyto-centrifuged onto glass slides. The cells were then stained with a polyclonal rabbit anti-rG-CSFR IgG (2.5 µg total) overnight at 4 °C and goat antirabbit IgG Dylight 488 (ThermoScientific) secondary antibodies and counterstained with Hoechst nuclear stain (ThermoScientific). Alternatively, the cells were stained using a naphthol AS-D chloroacetate specific esterase (NASDCl-esterase; Leder) kit (Sigma-Aldrich, St. Louis, Missouri, USA) according to the manufacturer's directions.

RNA and DNA isolation, cDNA synthesis, and quantitative gene expression analyses

For all experiments, tadpole and adult frog cells or tissues were homogenized in Trizol reagent (Invitrogen), flash frozen on dry ice, and stored at −80 °C until RNA and DNA isolation in accordance with manufacturer's directions. The isolated (phenol and chloroform extraction method) RNAs (500 ng total) were reverse transcribed into cDNAs using cDNA qscript supermix (Quantabio, Beverly, Massachusetts, USA), according to manufacturer's instructions.

DNA was isolated from the Trizol following RNA isolation. In brief, following phase separation and extraction of RNA, the remaining Trizol layer was mixed with back extraction buffer (4 M guanidine-thiocyanate, 50 mM sodium citrate, 1 M Tris pH 8.0) and centrifuged to isolate the DNA-containing aqueous phase. The DNA was precipitated overnight with isopropanol, pelleted by centrifugation, washed with 80% ethanol, and resuspended in TE buffer (10 mM Tris pH 8.0, 1 mM EDTA). DNA was then purified by phenol–chloroform extraction and resuspended in molecular grade water.

All quantitative analyses of *X. laevis* gene expression were performed using the CFX96 Real-Time System (Bio-Rad Laboratories, Hercules, California, USA) and iTaq Universal SYBR Green Supermix (Bio-Rad Laboratories). The Bio-Rad CFX Manager software (SDS) was employed for all expression analysis. All expression analyses were conducted using the ΔΔCt method relative to the *gapdh* endogenous control gene.

The FV3 and *Bd* loads were determined using absolute qPCR, performed on isolated DNA and using serially diluted FV3 or *Bd* standard curves. For FV3 DNA load analyses, an FV3 vDNA Pol

(ORF 60R) PCR fragment, cloned into the pGEM-T vector (Promega, Madison, Wisconsin, USA), and serially diluted to yield 10^8–10^1 vDNA Pol fragment-containing copies was used for FV3 DNA quantification. Amplification was performed using primers designed against the FV3 vDNA Pol gene. For *Bd* load analyses, the DNA isolated from enumerated *Bd* (10^7 zoospores) was serially diluted (10^7–10^2) and used as a standard curve for *Bd* quantification, using primers designed against the *Bd* ribosomal RNA internal transcribed spacer 1 (ITS1).

All primers were designed using the Integrated DNA Technologies (Research Triangle Park, North Carolina, USA) PrimerQuest Tool and validated in-house prior to use. Sequences of all employed primers are listed in Table 1 and denoted according to their respective functional roles.

Table 1. List of primer sequences.

Primer	Category	Sequence 5′ → 3′
arg1	c	TCCAAGGGACAGCCAAGAAG
	c	CTCGAACATCATTGCCAAATTC
Bd	*its1*	GCCATATGTCACGAGTCGAA
	its1	GCCAAGAGATCCGTTGTCA
csf1	b	GCCTCATATCATGCATCGTGGGAA
	b	TGTGTTCCGTGAAGCTGTCTCCTA
csf3	b	CCGACTGAACAAGGACATCAT
	b	TCTGTAGTCAGCAGTGTTTGAA
csf1r	a	GAGCAAGGGCACTGATAGTT
	a	AAAGGTCTACGGGCAAGATG
csf3r	a	TGGATGAAGGACTACAGCTAATG
	a	GCCTGTCATCTGTGAGGTTTA
cxcr1	a	CCAGTGGGTGTTTGGAATCT
	a	GCAAGGTATCGGTCAACACTAA
cxcr2	a	AGGATAGGGAGACACTTGGTAG
	a	GGCTGCTCTTGGTTTGATAGA
cxcr3 a	a	TGTTCCTTCTGGGAATGTTAGG
	a	GCCAGGTGTAGCAGAAAGAT
ela c, d	c, d	ATCTCCAAGAAGCCATTCTACC
	c, d	CACCTCCTGCACAGATCATATT
FV3 *vDNA pol*	—	CAAGAACGTGTGCTACTCCA
	—	AGCCTCTCGTACTCTACCTTC
gapdh control	—	GACACTCACTCCTCCATCTTTG
	—	TGCTGTAGCCGCATTCATTA
hdc	c, d	GAATCTGAAAGCTGGGAGAGAA
	c, d	GATGTCAGGGCAGGAAAGTAG

(*continued*)

Table 1. (*continued*)

Primer	Category	Sequence 5′ → 3′
ido	c, d	TATTGCGGATGCGAGAGTACA
	c, d	TCCCCGCTTTCTTGAACGTA
ifn7	g	TCTGTAGGAAGTCTCCGAAGTA
	g	CACA TTCAGTTGGAACCCTTTC
ifnx2	g	TCCATGCTTGTCTGCACAT
	g	ACCCTAGCACAGATGGGA
ifnx6	g	CAGTCCATCTCCTCACACTAAC
	g	CGCTTGATCCTGTGTCTTGTA
ifnx11	g	CATGCCAACAACTGGTTTCTC
	g	AATGCTGAGCCTCTGAAGATT
ifnx20 g	g	CATGGTGGTGCATACAGTCTAC
	g	CCTCCAGAAGGGAACGTAGATA
ifnl3	g	GTCCTTTCAGCGATGGGATAA
	g	ACGGCTTATGGCGAAACA
ifnl4	g	TCTGTAGGAAGTCTCCGAAGT
	g	CACA TTCAGTTGGAACCTTT
ifnlx1/2	g	TGACCACCTGGTTACCTACA
	g	CCAGGAATCTCATGTCCTCAATC
il4	b	GACATCAAGGACACCTGAAGAA
	b	GTCACAGGGAATCGGTACTAAAC
il10	b	TGCTGGATCTTAAGCACACCCTGA
	b	TGTACAGGCCTTGTTCACGCATCT
il34	b	TGATAAGCGATTGACCTACCTGGG
	b	AGCTCTTCTACGGTGATTCCTTGG
inos	c	TTGGCCTGAGGTATACGT
	c	CCCATGTACCAGCCGTTGA
kit	e	GAGGAAGCGGGATTCGTTTAT
	e	TCATTCCTTCACAGCCCATATC
lyz	c–e	GCACAGCTTTCTTTGAGAGTTC
	c–e	TACACCACCAACGACTGTTTA
mccpa	c, e	CTGGGCTTATCGAGTTTCTCTT
	c, e	GGCTTCCAACCTTGAGGATTA
mcpt1	e	TGCTCAGAACTTTACAGAACCA
	e	GCAGTCTCCTTTACCACCATAA
mhc1a	f	TGTGAAATGGGTGAAGAATGG

(*continued*)

Table 1. (*concluded*)

Primer	Category	Sequence 5′ → 3′
	f	GCTGCTGTGCTCCACATG
mhc2a	f	GGGCTGGAGAAATACACATCA
	f	CTGTACTGTTCCGGCTCTTT
mhc2b	f	GATGCTGGAGACAACCATTAAAC
	f	CTGGTTCCCAGTTCACAGATAC
mpo	c–e	CCAGAACCGAAGTGACTGTATC
	c–e	TGGCATCAACATAAGAGGTGAGA
noxa2	c	CAAACAACCCTCCTTCTCGTCCAA
	c	GGACCTGCATTTCTTCTGTCT
nox2	c	TAACATCTACCTCATGGCTGGGA
	c	CCAGTTTGGTCTGCCATACAAGGT
tnfa	b	TGTCAGGCAGGAAAGAAGCA
	b	CAGCAGAGCAAAGAGGATGGT
tpsab1	c–e	GTGCACCCTCGTTACAATAAATC
	c–e	GAAGCTGAAGGCACACAAAC

Note: Categories as follows: (a) immune receptors, (b) key growth factors and cytokines, (c) myeloid cell antimicrobial enzymes, (d) granulocyte and (e) mast cell-specific genes, (f) antigen presenting components, and (g) antiviral type I and III interferon cytokines.

Histology

All tadpole and adult frog tissues were immediately fixed in 10% neutral buffered formalin (VWR) upon excision. Tissues were processed and embedded in paraffin, sectioned (5 µm) and stained with hematoxylin and eosin, (NASDCl; specific)-esterase (Leder, Sigma-Aldrich), periodic acid-Schiff stain (PAS, Abcam, Cambridge, UK) or Toluidine blue stains (Sigma-Aldrich). All histology preparations and sectioning were performed by the GWU Pathology Core Lab. All histology stains were performed according to the respective manufacturers' instructions and optimized to frog or tadpole skin tissues when needed.

For staining of rCXCL8a-elicited skin granulocytes, the recovered cells were cyto-centrifuged onto glass slides and stained using a NASDCl-specific esterase kit (Sigma-Aldrich; according to manufacturer's directions) or with a HiTrap Protein A HP column (GE Health) and A Sulfo-Link Protein Kit (ThermoScientific) purified anti-rG-CSFR primary rabbit antibody (2.5 µg total) overnight at 4 °C. The following day the cells were stained with a goat antirabbit IgG Dylight 488 (ThermoScientific) secondary antibodies (1 h) and counterstained with Hoechst nuclear stain (ThermoScientific).

Statistical analyses

Statistical analyses of the gene expression and NASDCl-esterase and metachromatic-granule (Toluidine blue) cell counts data were conducted using paired Student's *t*-tests. Chemotaxis data were examined using ANOVA and Tukey's post hoc tests via GraphPad Prism 7.0 software. Alpha level was set at 0.05; p values <0.05 were considered statistically significant.

Results

Tadpole and adult *X. laevis* possess resident skin granulocytes, which are not mast cells

In examination of healthy *X. laevis*, we observed esterase-positive cells, indicative of granulocyte-lineage cells (Braun et al. 1996) in the epidermal layers of both tadpole and adult *X. laevis* (**Fig. 1**). To discern whether these tadpole and adult *X. laevis* esterase-positive skin cells were mast cells, we stained serial skin sections with either the NASDCl-specific esterase stain, identifying granulocyte-lineage cells or Toluidine blue stain, highlighting metachromatic mast cell granules (Schueller et al. 1967; Johnson and Moran 1974). While the tadpole esterase-positive cells were observed almost exclusively in the epidermal layers of the tadpole skin or associated with their basement membranes (Figs. **1A** and **1Ai**), cells possessing metachromatic granules (Johnson and Moran 1974; Tas 1977; Ingaleshwar et al. 2016; Puebla-Osorio et al. 2017) were found entirely in the lower dermal layers of the corresponding serial skin sections (**Figs. 1B** and **1Bi**). A similar localization pattern was revealed in adult *X. laevis*, wherein esterase-positive granulocytes were observed within their epidermal layers (**Figs. 1C** and **1Ci**), and metachromatic cells were seen exclusively in the lower dermal skin layers (**Figs. 1D** and **1Di**). We did not observe colocalization or overlap of esterase-positive and metachromatically stained cells across any of the examined tadpole or adult frog skin tissues.

Tadpole and adult *X. laevis* resident skin granulocytes migrate towards rCXCL8a and rCXCL8b and possess characteristic granulocyte morphology

Because tadpoles and adult *X. laevis* express *cxcl8a* and *cxcl8b* in their skin (Koubourli et al. 2018), we reasoned that CXCL8a and CXCL8b may be playing a role in the homing or retention of the observed esterase-positive granulocytes within these animals' skin tissues. As an extension of this reasoning, we examined whether we could chemo-attract the esterase-positive granulocytes out of the *X. laevis* skin tissues using recombinant rCXCL8a and rCXCL8b via Boyden chemotaxis chambers. As expected, both rCXCL8a and rCXCL8b elicited chemo-attraction of cells out of the tadpole and adult *X. laevis* skin sections (**Fig. 2**). The optimal dose for recruiting cells out of tadpole and adult skin sections was 10^{-4} ng/mL for both rCXCL8a and rCXCL8b (**Figs. 2A** and **2B**).

We confirmed that the observed skin granulocyte migration was chemotaxis-mediated (involving cell movement along a gradient) and not due to chemokinesis (changes in cell movement in a gradient-independent manner; Rikitake and Takai 2011). To this end, the same migration assays were conducted with the following alteration: 10^{-4} ng/mL (optimal doses) of rCXCL8a or rCXCL8b were loaded in both upper and lower Boyden chambers, thereby abolishing the chemokine gradient. If the observed cell migration was due to chemokinesis, we would expect to still see greatly increased cell migration despite the abolished gradient. Rather, this resulted in significant reduction of the tadpole and adult frog skin granulocyte migration (as compared to 10^{-4} ng/mL in the bottom chamber only, **Figs. 3A** and **3B**). The rCXCL8a- and rCXCL8b-elicited chemotaxis was dependent on CXCR1/2, as pharmacological antagonism of these chemokine receptors with reparixin significantly reduced chemotaxis of tadpole and adult frog skin granulocytes towards rCXCL8a or rCXCL8b (10^{-4} ng/mL; **Figs. 2C** and **2D**).

The tadpole and adult frog skin cells chemoattracted to rCXCL8a and rCXCL8b exhibited characteristic granulocyte polymorphous nuclei and surface staining of the G-CSFR granulocyte marker (**Fig. 3**). The migrating cells also exhibited positive but variable esterase activity (Leder stain; **Fig. 3**). There were no notable differences between tadpole and adult *X. laevis* rCXCL8a- or

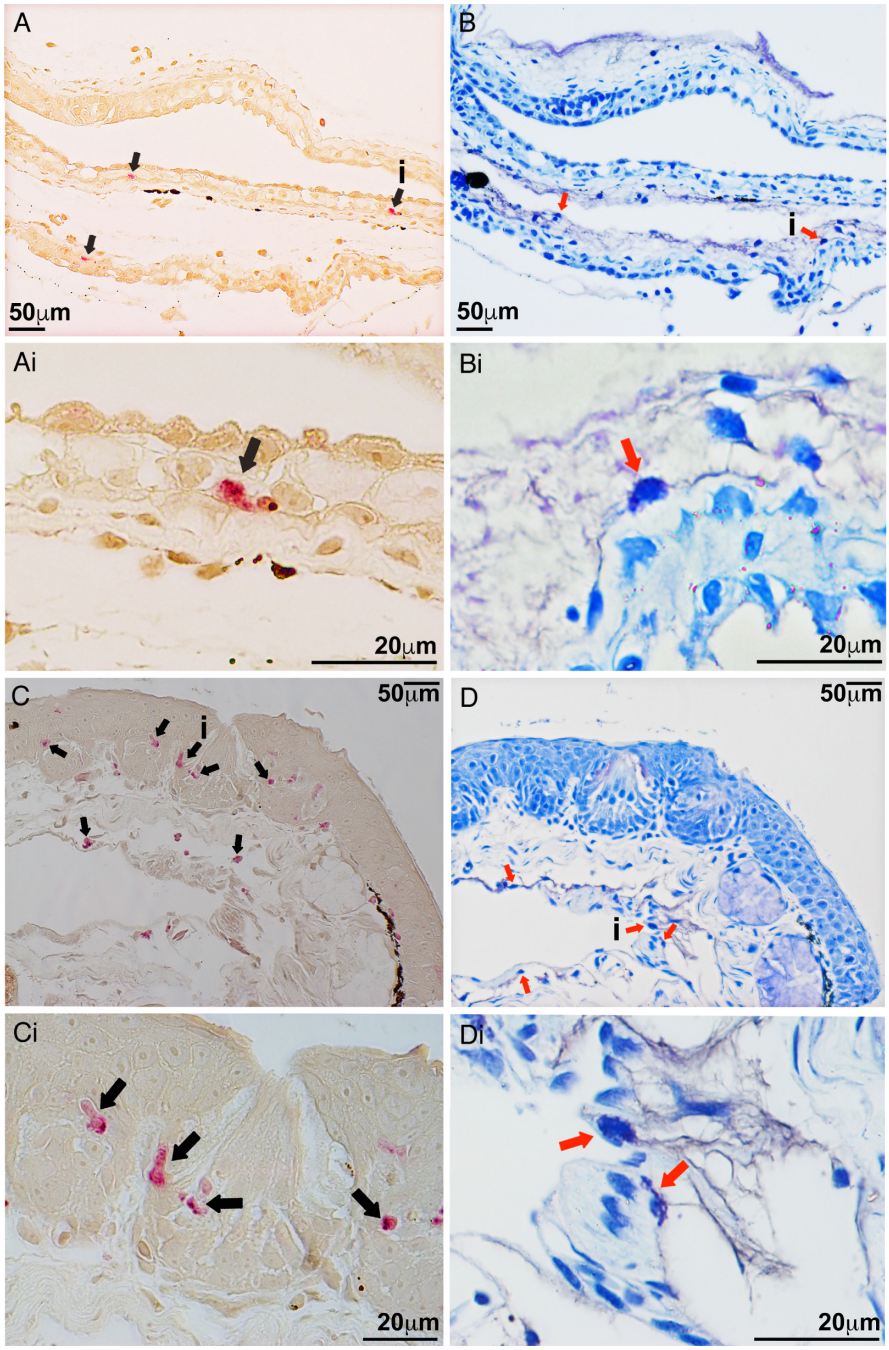

Fig. 1. Tadpole and adult *Xenopus laevis* possess nonmast cell granulocytes in their skin epidermis. The skins of healthy tadpoles (A and B; stage NF 54) and adult frogs (C and D; ~1 year old) were fixed in 10% neutral buffered formalin, embedded in paraffin, serially sectioned and examined for the presence of granulocytes and mast cells via NASDCl-specific esterase (Leder stain; A, C) and Toluidine blue (B, D) stains, respectively. (Ai), (Bi), (Ci), and (Di) are magnified images of cells indicated by "i" in respective (A)–(D) panels. Esterase-positive and metachromatic cells are indicated by arrows. These results are representative of two independent histological studies, each performed using the skins of three individual animals ($N = 6$).

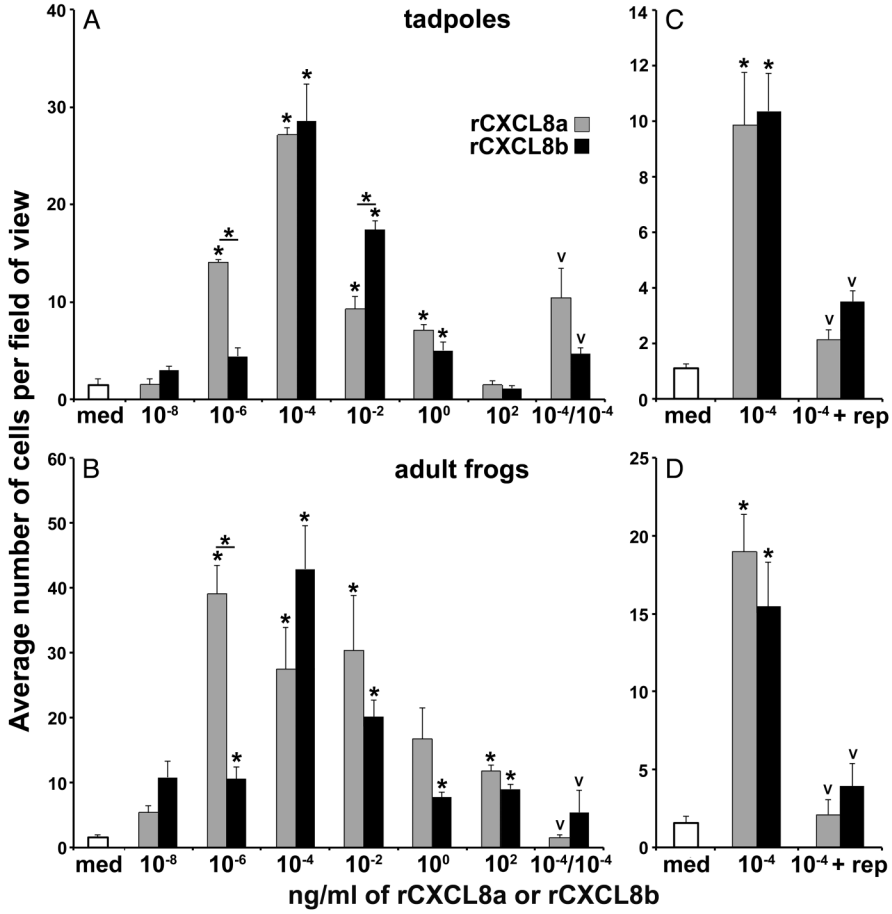

Fig. 2. Skin-resident tadpole and adult granulocytes are chemo-attracted by rCXCL8a and rCXCL8b. Chemotaxis assays were performed against medium alone (med) or 10^{2}–10^{-8} ng/mL of rCXCL8a or rCXCL8b in bottom Boyden chamber wells, with tadpole (A, C) or adult frog (B, D) skin sections (5 mm^2; $N = 3$–6 per chemokine concentration) loaded into top wells, separated by chemotaxis filters. After incubation the bottom faces of the filters were stained with Giemsa stain and examined for numbers of migrating cells (40× objective). Chemokinesis experiments were performed using 10^{-4} ng/mL of rCXCL8a or rCXCL8b (the most chemo-attractive concentration) in both bottom and the top chemotaxis chambers. The reparixin (CXCR1/2 inhibitor; MedChemExpress) studies (C, D) were carried out by loading 10^{-4} ng/mL (optimal doses) of rCXCL8a or rCXCL8b to bottom chemotaxis chambers and tadpole or adult skin sections (5 mm^2) in conjunction with reparixin (1 nM final) in the upper chambers. Asterisks (*) denote statistically significant difference in cell migration relative to medium; asterisks above lines (*) denotes statistical differences in the migration activity between the treatment groups denoted by the line and (v) denotes a statistical decrease in respective migration relative to 10^{-4} ng/mL of either rCXCL8a or rCXCL8b alone, $p < 0.05$.

rCXCL8b-chemoattracted skin granulocytes (Fig. 3) nor were cells with metachromatic granules from Toluidine blue staining detected in any of the cells derived by this approach.

Tadpole and adult *X. laevis* resident skin granulocytes express key immune effector genes

To further characterize the tadpole and adult skin granulocytes, we isolated the respective cells by the chemotaxis methods described above and examined their expression of a panel of immune genes.

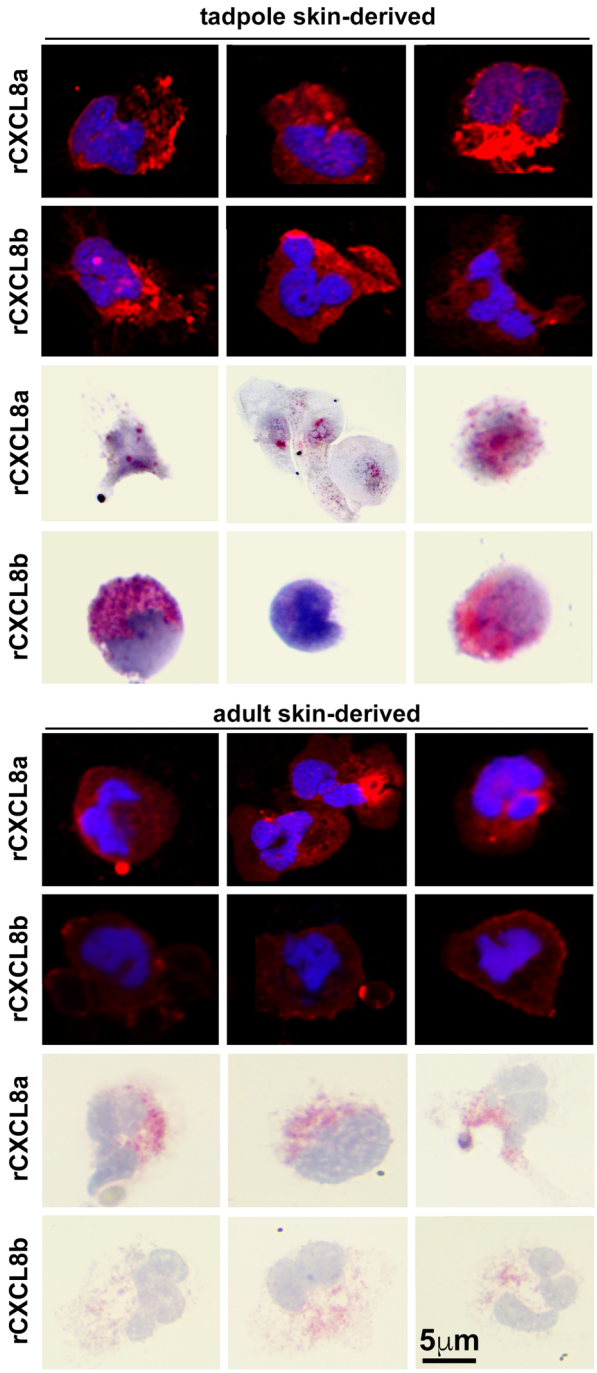

Fig. 3. Tadpole and adult rCXCL8a- and rCXCL8b-chemoattracted cells are polymorphonuclear granulocytes that express surface G-CSFR. Chemotaxis assays were performed on tadpole and adult skin sections (5 mm^2) using rCXCL8a or rCXCL8b (10^{-4} ng/mL). Cells that migrated to the bottom Boyden chamber wells were combined, cyto-centrifuged onto slides and examined for surface G-CSFR expression (1st, 2nd, 5th, and 6th rows; polyclonal anti-rG-CSFR primary rabbit antibody and goat anti-rabbit IgG Dylight 488 secondary antibody) and esterase (Leder stain: 3rd, 4th, 7th, and 8th rows) activity. The presented results are representative of two independent experiments using six tadpoles or adult *X. laevis*, each.

Our preliminary analyses did not yield discernable differences between the transcriptional profiles of tadpole rCXCL8a- and rCXCL8b-attracted skin granulocytes or between adult frog skin granulocytes derived by rCXCL8a and rCXCL8b. Accordingly, we chose to perform subsequent gene expression analyses on tadpole and adult skin granulocytes that migrated towards rCXCL8a and compared the immune gene expression of these cells to tadpole or adult frog rG-CSF-derived granulocytes isolated from these animals' peritonea (Figs. 4–6).

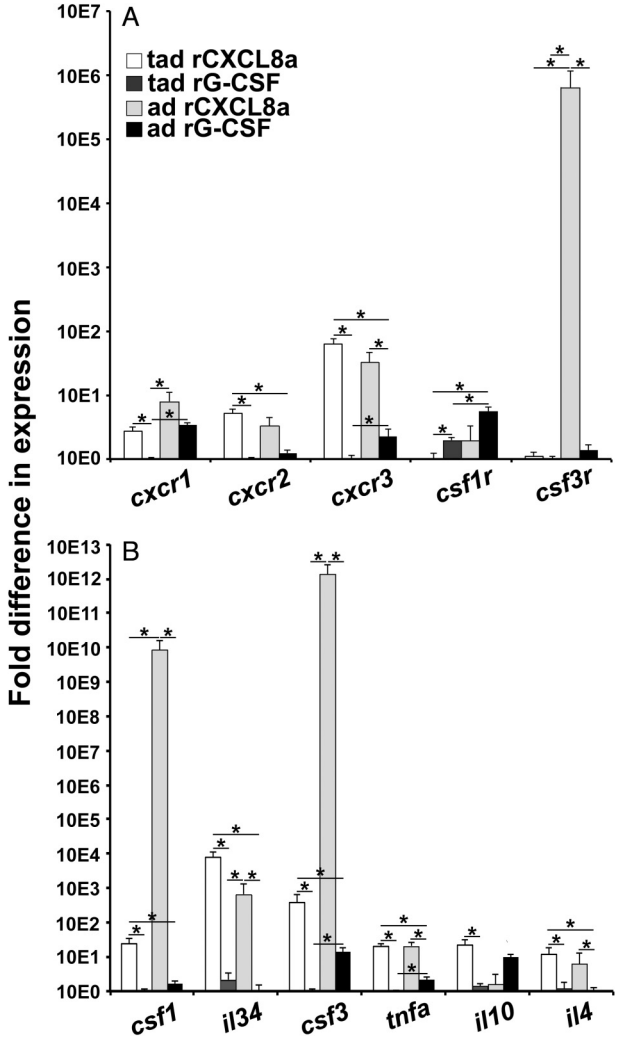

Fig. 4. Analyses of tadpole and adult *Xenopus laevis* skin-resident granulocyte expression of innate immune cell receptors, growth factors, and cytokine genes. Chemotaxis assays were performed on tadpoles (tad) and adult frog (ad) skin sections (5 mm^2; $N = 5–6$/life stage) using the optimal chemotaxis dose of rCXCL8a (10^{-4} ng/mL). Cells that migrated to the bottom Boyden chamber wells were collected and compared by qPCR to tadpole and adult frog peritoneum-derived rG-CSF-granulocytes for their expression of (A) immune receptors and (B) key growth factors and cytokines. All gene expression was quantified relative to the *gapdh* endogenous control and normalized against the lowest expressing cell type for each gene, which was set at (10E0). The results are means ± SE and asterisks (*) above lines denote statistical gene expression differences between the cell types denoted by the respective lines, $p < 0.05$.

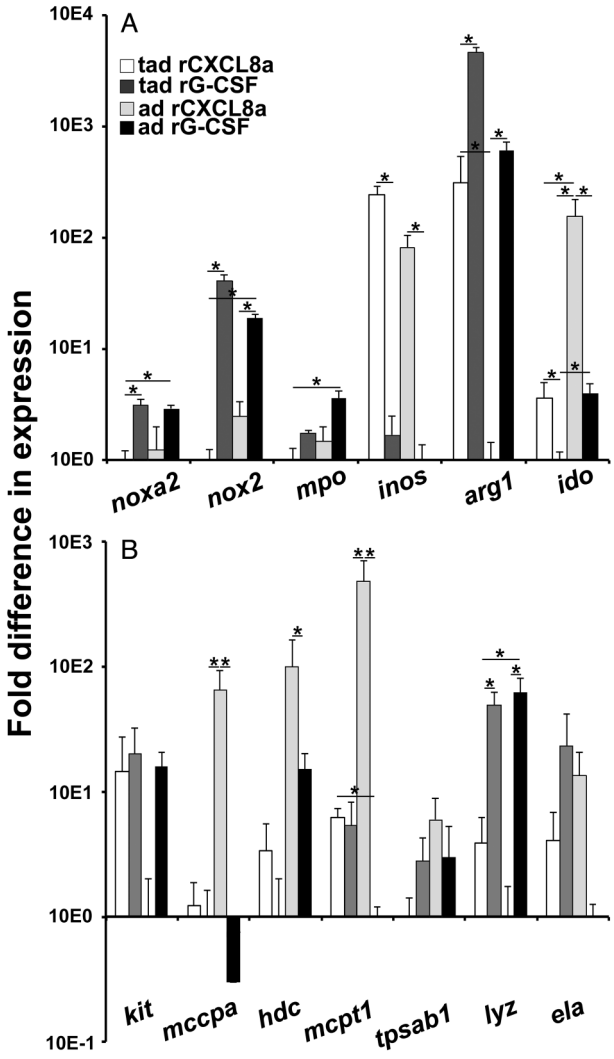

Fig. 5. Analyses of tadpole and adult *Xenopus laevis* skin-resident granulocyte expression of antimicrobial enzymes, mast cell- and granulocyte-specific genes. Chemotaxis assays were performed on tadpoles (tad) and adult frog (ad) skin sections (5 mm^2; $N = 5–6$/life stage) using the optimal chemotaxis dose of rCXCL8a (10^{-4} ng/mL). Cells that migrated to the bottom Boyden chamber wells were collected and compared by qPCR to tadpole and adult frog peritoneum-derived rG-CSF-granulocytes for their expression of (A) antimicrobial enzymes, (B) mast cell and granulocyte-specific genes. All gene expression was quantified relative to the *gapdh* endogenous control and normalized against the lowest expressing cell type for each gene, which was set at (10E0). The results are means ± SE and asterisks (*) above lines denote statistical gene expression differences between the cell types denoted by the respective lines, $p < 0.05$.

Tadpole and adult skin-derived granulocytes exhibited significantly greater gene expression of *cxcr1*, *cxcr2*, and *cxcr3* chemokine receptors but lower expression of *csf1r* macrophage growth factor receptor compared to the respective peritoneum-derived rG-CSF-granulocyte populations (Fig. 4A). While tadpole skin granulocyte expression of the *csf3r* granulocyte growth factor receptor gene was comparable to that of tadpole rG-CSF-granulocytes, adult frog skin granulocytes had substantially greater *csf3r* mRNA levels than that of adult frog rG-CSF-granulocytes (Fig. 4A).

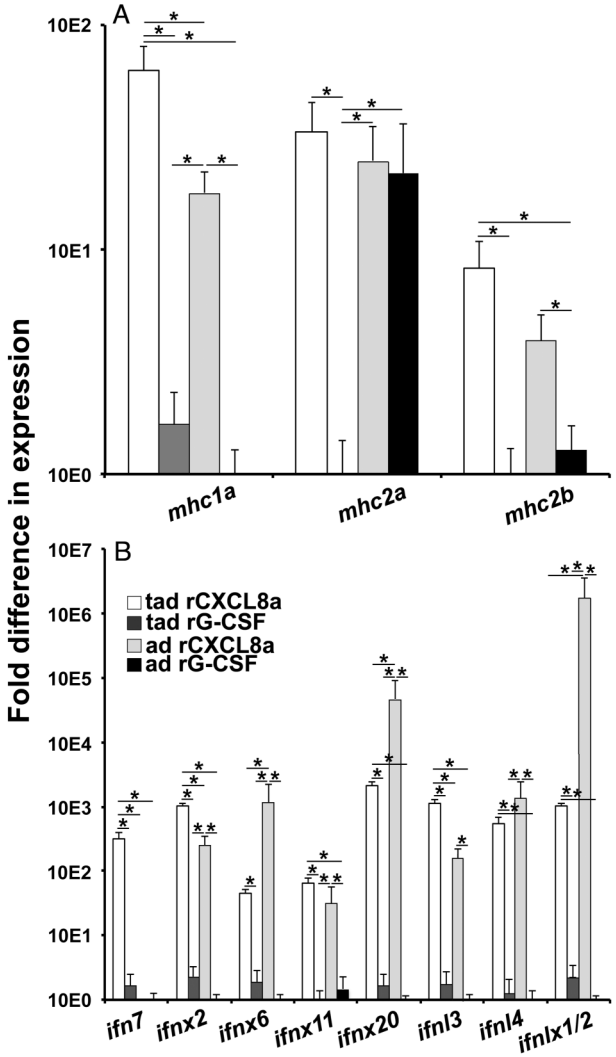

Fig. 6. Analyses of tadpole and adult *Xenopus laevis* skin-resident granulocyte expression of antigen presentation and antiviral IFN cytokine genes. Chemotaxis assays were performed on tadpole (tad) and adult (ad) skin sections (5 mm^2; $N = 5–6$/life stage) using the optimal chemotaxis dose of rCXCL8a (10^{-4} ng/mL). Cells that migrated to the bottom Boyden chamber wells were collected and compared by qPCR to tadpole and adult frog peritoneum-derived rG-CSF-granulocytes for their expression of (A) antigen presenting components and (F) antiviral type I and III interferon cytokine genes. All gene expression was quantified relative to the *gapdh* endogenous control and normalized against the lowest expressing cell type for each gene, which was set at (10E0). The results are means ± SE and asterisks (*) above lines denote statistical gene expression differences between the cell types denoted by the respective lines, $p < 0.05$.

Gene expression of *csf1*, *il34*, and *csf3* myeloid cell growth factors was significantly greater in tadpole and adult frog skin granulocytes compared to the corresponding peritoneum-derived rG-CSF-granulocyte populations (Fig. 4B). Moreover, tadpole and adult frog skin granulocytes possessed significantly more transcripts for the proinflammatory tumor necrosis factor-alpha (*tnfa*) and the Th2 interleukin-4 (*il4*) cytokines than the respective rG-CSF-granulocyte populations (Fig. 4B). Tadpole but not the adult skin granulocytes also possessed greater gene expression of the immunosuppressive interleukin 10 (*il10*) cytokine than the rG-CSF-granulocytes (Fig. 4B).

Gene expression analysis of key antimicrobial enzyme genes revealed that tadpole and adult frog skin granulocytes exhibited fewer transcripts of the NADPH oxidase (catalytic subunits *noxa2* and *nox2*), myeloperoxidase (*mpo*), and arginase-1 (*arg1*) enzymes but significantly greater transcripts for the inducible nitric oxide synthase and indoleamine 2,3-dioxygenase (*ido*) compared with their respective rG-CSF-granulocytes (**Fig. 5A**).

We next examined expression of hallmark mast cell-specific genes (mast/stem cell growth factor receptor (*kit*), mast cell carboxypeptidase (*mccpa*), histidine decarboxylase (*hdc*), mast cell protease 1 (*mcpt1*), and beta tryptase (*tpsab1*)) and genes associated with neutrophil granulocytes (lysozyme (*lyz*) and elastase (*ela*)) across the skin- and peritoneum-derived granulocyte populations. Of particular note from the mast cell-associated gene analysis, the adult (but not tadpole) skin granulocytes expressed greater levels of *mccpa* and *mcpt1*, whereas both tadpole and adult frog skin granulocytes possessed greater transcript levels for *hdc* when compared with the respective rG-CSF-granulocytes (**Fig. 5B**). Conversely, tadpole and adult frog rG-CSF-granulocytes exhibited greater gene expression of *lyz*, and adult (but not tadpole) rG-CSF-granulocytes possessed greater mRNA levels for *ela* (**Fig. 5B**).

In consideration of these skin granulocytes as possible sentinels of this tissue, we also examined their expression of antigen presenting genes *mhc1a*, *mhc2a*, and *mhc2b*. Tadpole and adult *X. laevis* skin granulocytes exhibited greater gene expression of *mhc1a* and *mhc2b* than the respective tadpole or adult rG-CSF-granulocytes (**Fig. 6A**). Tadpole (but not adult) skin granulocytes also possessed greater *mhc2a* transcript levels than the corresponding rG-CSF-granulocyte population (Fig. **6A**).

We recently demonstrated that tadpoles and adult frogs undergo substantial and disparate skin type I and type III antiviral interferon (IFN) responses to the Frog Virus 3 ranavirus (Wendel et al. 2017, 2018). To evaluate tadpole and adult frog skin granulocytes as possible sources of these antiviral IFNs, we examined these cells for their expression of representative (based on phylogeny; Sang et al. 2016; Wendel et al. 2017) intronless and intron-containing type I and III IFN genes (*ifn, ifnx, ifnl, ifnlx*, respectively) in comparison with tadpole or adult rG-CSF-granulocytes. With the exception of *ifn7*, tadpole and adult skin granulocytes exhibited substantially more robust expression of all examined type I (*ifnx2*, *ifnx6*, *ifnx11*, *ifnx20*) and type III (*ifnl3*, *ifnl4*, *ifnlx1/2*) IFN genes than the respective rG-CSF-granulocyte populations (Fig. **6B**). Moreover, tadpole (but not adult) skin granulocytes had greater mRNA levels of *ifn7* than observed in the rG-CSF-granulocytes (**Fig. 6B**).

Altering the skin granulocyte populations affects tadpole susceptibility to FV3

Since both tadpoles and adult *X. laevis* express *cxcl8a* and *cxcl8b* in their skin (Koubourli et al. 2018) and rCXCL8a and rCXCL8b chemo-attracted specific esterase-positive granulocytes out of both tadpole and adult skin tissues, we sought to explore the relationship between these chemokines and the skin granulocytes in vivo. To this end, we injected *X. laevis* tadpoles subcutaneously with rCXCL8a or rCXCL8b, which resulted in substantial accumulation of esterase-positive cells in the epidermal and dermal skin layers of these animals (**Figs. 7A–7C** and **7E**) but had no effect on the numbers of metachromatic granule-containing cells. Moreover, inhibiting the tadpole rCXCL8a/b receptors, CXCR1/CXCR2, with the reparixin pharmacological antagonist (rep; Pawlick et al. 2016) significantly diminished the numbers of esterase-positive cells within the tadpole skin (**Figs. 7D** and **7E**) but had no observable effect on the numbers of skin metachromatic granule-containing cells.

The Frog Virus 3 (FV3) ranavirus afflicts anuran tadpoles to a greater extent than the adult frogs with the tadpole skin representing an important tissue for viral entry (Carey et al. 1999; Wendel et al. 2017, 2018). Accordingly, to discern the roles of the tadpole skin granulocytes during FV3 infections, we enriched tadpole skin granulocytes by subcutaneous injections with either rCXCL8 isoform or ablated

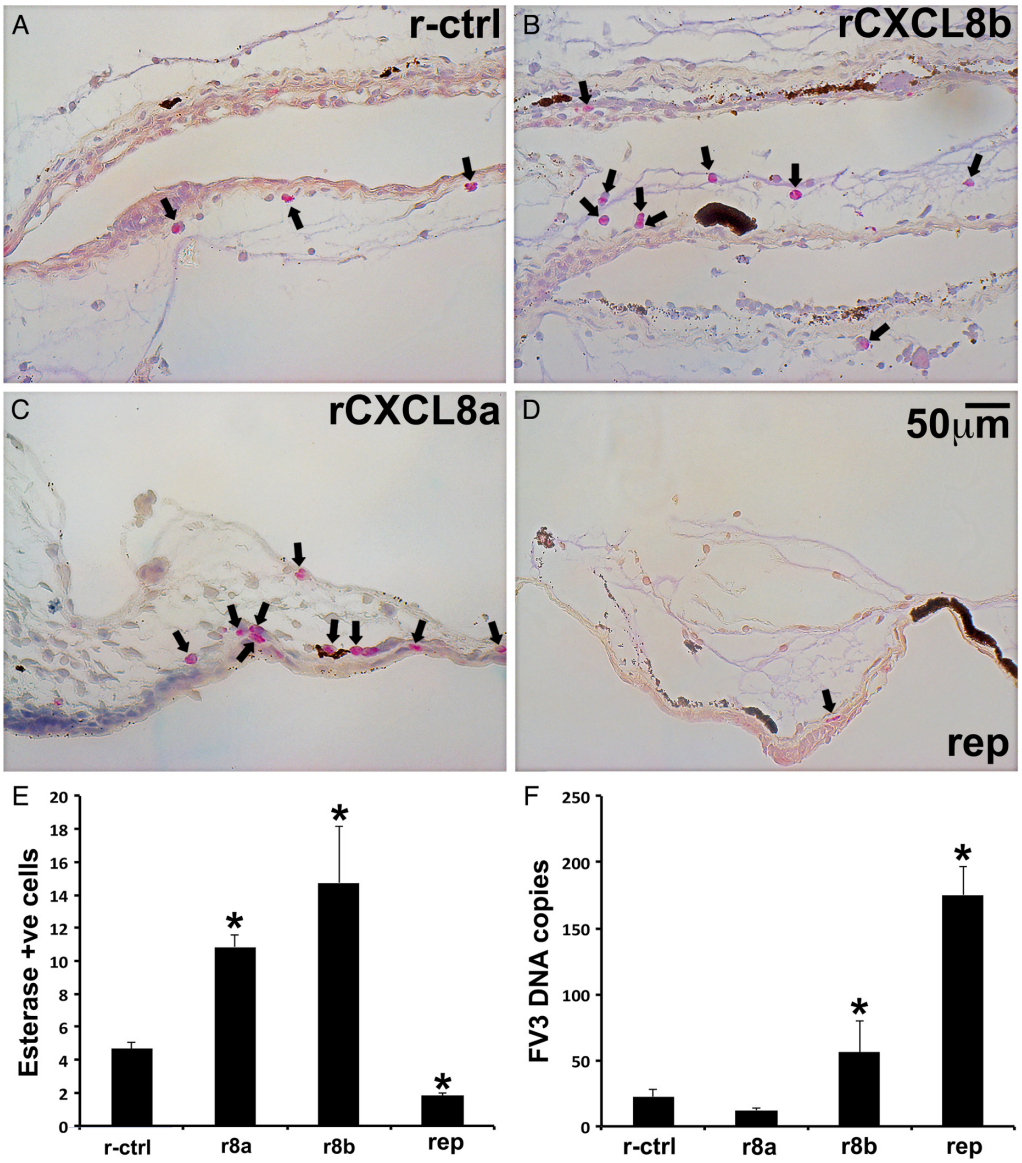

Fig. 7. Altering the skin granulocyte populations affects tadpole susceptibility to Frog virus 3 (FV3). Tadpoles were injected subcutaneously with r-ctrl, 500 ng of rCXCL8a or rCXCL8b or reparixin (rep, 50 mg/kg) and (A–D) examined by NASDCl-specific esterase (Leder) stain. Arrows indicate esterase-positive cells, presented in (E) as means ± SE for 5–6 tadpoles per treatment group ($N = 5–6$). After altering the numbers of skin esterase-positive cells, (F) tadpoles were infected by water bath with FV3 (1×10^6 PFU) for 24 h and the tadpole dorsal skins were examined for FV3 DNA loads by absolute qPCR and presented as means ± SE. Asterisks (*) denote statistical differences from r-ctrl administered tadpoles, $p < 0.05$.

the numbers of these cells with reparixin, as above (Figs. 7A and 7E). We then challenged the tadpoles with FV3 by water bath and examined their FV3 loads. Tadpoles that were enriched for skin granulocytes by subcutaneous administration of rCXCL8b (but not rCXCL8a) possessed significantly greater skin FV3 loads than the r-ctrl or rCXCL8a-treated animals (Fig. 7F). Moreover, tadpoles with pharmacologically reduced skin granulocyte populations possessed even greater FV3 loads in their skin tissues than rCXCL8b-skin granulocyte-enriched or control animals (Fig. 7F).

Altering the skin granulocyte populations affects adult *X. laevis* susceptibility to *Bd*

Subcutaneous injections of adult frogs with rCXCL8a or rCXCL8b significantly increased esterase-positive cells in both their epidermal and dermal skin layers (Figs. 8A–8C and 8E), whereas metachromatic granule-containing skin cell populations were not affected by these treatments. Consistent with these findings, reparixin treatment significantly diminished the esterase-positive (but not metachromatic) cells within adult frog skins (Figs. 8D and 8E).

As *B. dendrobatidis* predominately afflicts anuran adults by colonizing their skin (Skerratt et al. 2007), we explored whether perturbing skin granulocyte populations as above would alter animal susceptibility to *Bd*. Adult frogs with skin-granulocytes enriched by rCXCL8b possessed significantly greater *Bd* loads than detected in rCXCL8a-treated or control animals (Fig. 8F). However, unlike tadpole susceptibility to FV3, adult frog susceptibility to *Bd* was not altered by reparixin-mediated reduction of their skin granulocytes (Figs. 7F and 8F, respectively). Our histological analyses confirmed the presence of *Bd* zoosporangium, most with discharged papillae, within the skins of adult frogs and often accompanied by extensive thickening of epidermal layers (Fig. S1).

Discussion

As an aquatic species, *X. laevis* skin must support gas, water, and ion exchange as well as serve as a physical barrier against myriad pathogens present in their environments (Feder and Burggren 1992). In turn, the global amphibian declines highlight the urgency to better understand their cutaneous immune components. To this end and through the present work, we identified resident granulocyte populations in the skin tissues of tadpole and adult *X. laevis*, bearing some but not all hallmark characteristics of mast cells. We further demonstrated that these cells have a role in the anti-viral and anti-bacterial properties of *X. laevis* skin.

The *X. laevis* skin-resident polymorphonuclear granulocytes, confirmed by their esterase activity (Braun et al. 1996), described here do not possess the defining metachromatic staining, a defining feature of mast cells and occupy distinct layers of the skin from the what appear to be more conventional mast cells. Nonetheless, these skin granulocytes did express notable levels of several mast cell markers compared with more conventional (i.e., peritoneum-derived) granulocytes. Indeed, both tadpole and adult *X. laevis* skin granulocytes expressed significant mast cell carboxypeptidase, used as a marker of zebrafish mast cells (Dobson et al. 2008) and histidine decarboxylase. To our knowledge, the only granulocyte-lineage cells thought to reside in the tissues of healthy vertebrates are mast cells, although other granulocyte-lineage cells, namely neutrophils and basophils, readily infiltrate infected and (or) inflamed skin tissues of more recently diverged vertebrates (Minnicozzi et al. 2011; Rigby and DeLeo 2012). It seems probable that amphibian skin-resident immune populations, as dictated by their unique physiology and environments, may be distinct to those that are characteristic of terrestrial vertebrates. In fact, the aquatic vertebrates studied to date have considerably fewer mast cells (possessing metachromatic granules) as compared with animals that exist mostly or entirely on land (Baccari et al. 2011). The presence of specialized, skin-resident amphibian immune cell population(s) is especially appealing given the paucity of knowledge surrounding aquatic vertebrate hematology and immunity combined with the fact that these animals are in constant contact with millions of viruses, bacteria, fungi, and protozoans via their skin. Both tadpole and adult *X. laevis* skin granulocytes express significant levels of *mhc1a* and *mhc2b* compared with the more conventional tadpole and adult frog peritoneum-derived G-CSF-granulocytes, which supports the notion that these skin-resident granulocytes may serve as immune sentinels of these tissues.

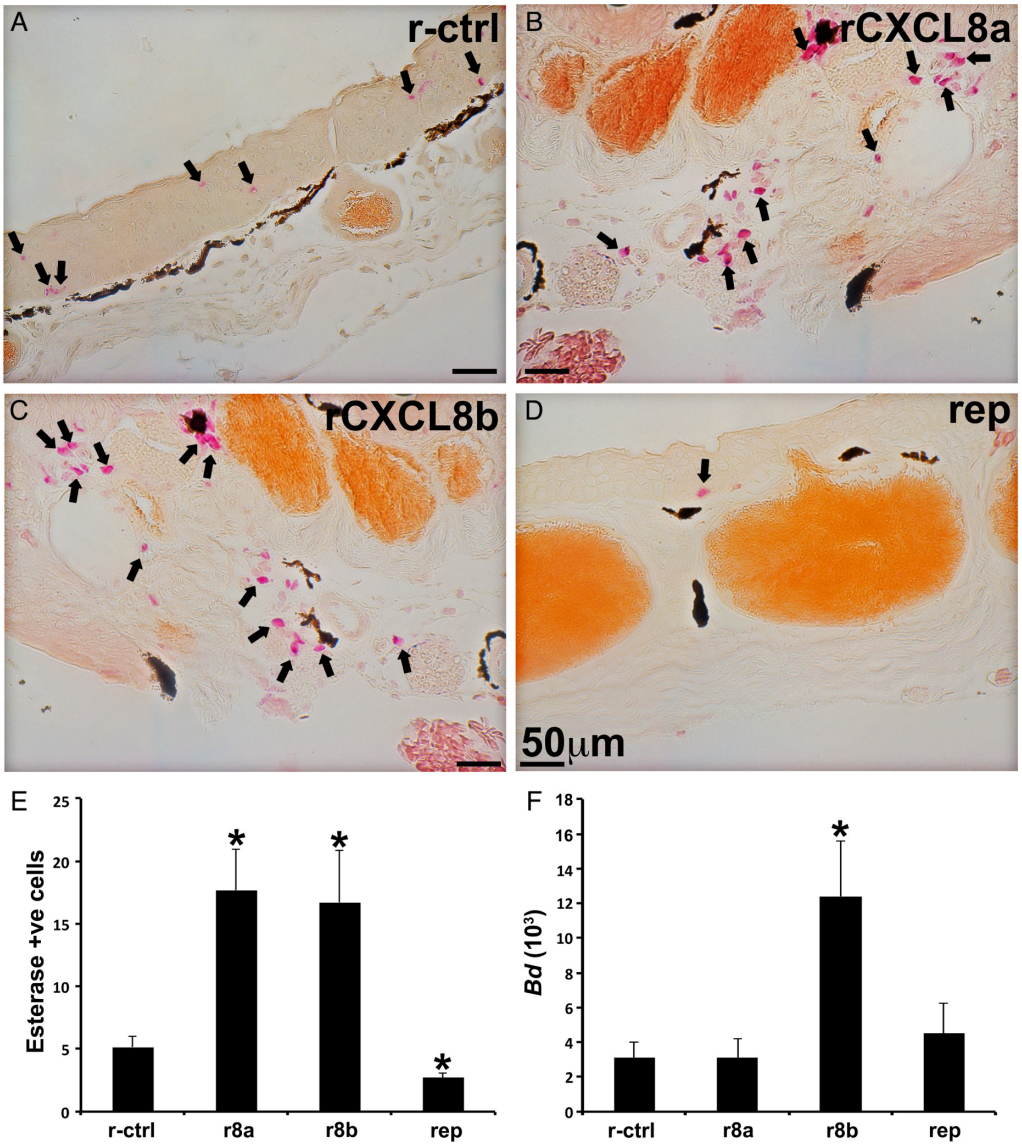

Fig. 8. Altering adult frog skin granulocyte populations affects their susceptibility to *Batrachochytrium dendrobatidis* (*Bd*). Adult *Xenopus laevis* were injected subcutaneously with r-ctrl, 2.5 μg of rCXCL8a or rCXCL8b or reparixin (rep, 50 mg/kg) and (A–D) examined by NASDCl-specific esterase (Leder) stain. Arrows indicate esterase-positive cells, presented in (E) as means ± SE for 5–6 frogs per treatment group ($N = 5–6$). After altering the skin esterase-positive cells, (F) frogs were infected by water bath with *Bd* (10^7 zoospores). Seven days postinfection the frog dorsal skins were examined for *Bd* loads by absolute qPCR and presented as means ± SE. Asterisks (*) denote statistical differences from r-ctrl administered frogs, $p < 0.05$.

In light of their unique habitats and physiologies, it is entirely fathomable that amphibians would possess disparate granulopoietic strategies to those of terrestrial vertebrates. Notably, the differentiation of mammalian mast cells as well as the developmentally related basophils is attributed to the function of interleukin-3 (IL-3) and stem cell factor (SCF; Kit ligand) cytokines (Varricchi et al. 2018). *Xenopudinae* amphibians are thought not to encode any of the IL-5 family members, including

IL-3, IL-5, or granulocyte/macrophage colony-stimulating factor (GM-CSF, CSF-2; Wang and Secombes 2015). And while IL-3 and SCF appear to be more important to the development of basophil and mast cells, respectively (Varricchi et al. 2018), the absence of IL-5 family members in amphibians suggests their granulopoiesis may indeed be distinct from that of more recently diverged vertebrates.

Mast cells are thought to arise from common granulocyte or macrophage precursor (GMP) cells in both mammals and fish (Dobson et al. 2008; Qi et al. 2013) and thus, depend on G-CSF (CSF-3) as a growth factor at some point during their commitment, differentiation and (or) egress from their species-specific designated hematopoietic organs. Indeed, although SCF has been more prominently implicated in mast cell development, G-CSF has also been shown to promote the expansion of mammalian mast cells (Ulich et al. 1991; Yang et al. 1999). The expression of cell-surface G-CSFR on *X. laevis* tadpole and adult skin granulocytes confirms their granulocyte lineage but does not permit us to clearly speculate on the relationships between these frog cells and the mammalian mast cells or other granulocyte subsets. However, when compared with more conventional, peritoneum-derived tadpole and adult frog granulocytes, these skin granulocytes exhibited gene expression more akin to, and characteristic of, mammalian mast cells. This includes greater skin granulocyte expression of interleukin-4 (IL-4), mast cell carboxypeptidase, and histidine decarboxylase, all of which are associated with mammalian mast cells (Metcalfe et al. 1997; Varricchi et al. 2018). Conversely, gene expression of the SCF receptor (*kit*), a hallmark of mammalian mast cells (Metcalfe et al. 1997), did not differ significantly between the tadpole skin and conventional granulocytes, but it was nearly absent in the adult frog skin-derived cells. Thus, the skin granulocytes described here may be distinct from mammalian mast cells, at least insofar as their low *kit* expression and thus independence of SCF.

Whereas more recently diverged vertebrates encode a single CXCL8 (IL-8) chemokine, possessing the Glu-Leu-Arg (ELR) motif that is characteristic of mammalian proinflammatory chemokines (Clark-Lewis et al. 1991, 1993), we recently demonstrated that amphibians possess two distinct CXCL8 forms, CXCL8a and CXCL8b. The former isoform participates in inflammatory responses, while the latter recruits granulocytes bearing immunosuppressive gene expression (Koubourli et al. 2018). During those studies, we also observed prominent expression of both CXCL8 isoforms in the skins of tadpoles and adult frogs and demonstrated that both chemokine isoforms recruited tadpole and adult granulocytes by engaging CXC chemokine receptors, CXCR1 and CXCR2 (Koubourli et al. 2018). Our present work indicates that the tadpole and adult skin granulocytes are chemoattracted towards CXCL8a and CXCL8b in vitro and in vivo, while pharmacological inhibition of the CXCR1/2 significantly diminishes the numbers of tadpole and adult skin granulocytes. Taken together, these data support the notion that CXCL8a and CXCL8b mediate the homing and (or) retention of these skin granulocyte populations. Notably, homing of mammalian mast cell precursors to the skin depends on CX_3CR1 (Papadopoulos et al. 2000), whereas homing of mammalian mast cells to mucosal tissues depends on the activation of CXCR2 (Gurish et al. 2001; Abonia et al. 2005). To our knowledge, homologs of CX_3CR1 or its ligand (CX_3CL1) have not been identified or annotated in *Xenopudinae* genomes. It is however interesting to consider that while the amphibian skin is also a mucosal tissue, the tadpole and adult frog skin granulocytes described here appear to be dependent on the CXCL8-CXCR1/2 axis for their presence in the skin tissues.

Our results indicate that enriching tadpole and adult skin granulocytes with rCXCL8b renders them more susceptible to FV3 and *Bd*, respectively. This is consistent with our past results that suggest that CXCL8b chemoattracts granulocytes bearing immunosuppressive characteristics. Since both CXCL8a and CXCL8b are expressed in the skin tissues of tadpoles and adults, we speculate that these chemokines may mediate the homing of functionally distinct granulocyte subsets. Given our past

work demonstrating *X. laevis* CXCL8a and CXCL8b both function through CXCR1 and CXCR2 (Koubourli et al. 2018), distinct tadpole and adult frog CXCL8a- and CXCL8b-recruited skin granulocyte subpopulations will also likely possess both CXCR1 and CXCR2 receptors. Because the ELR motif is present only on the *X. laevis* CXCL8a isoform and is important to inflammatory chemokine-receptor interactions (Cai et al. 2009), we postulate that the inflammatory and immunosuppressive frog granulocyte populations are recruited towards CXCL8a and CXCL8b, respectively, as a result of distinct ligand-CXCR1/2 receptor interactions. However, since both chemokines act through CXCR1 and CXCR2, if there are multiple granulocyte populations in the frog skin, they would express both receptors. Thus, without a greater understanding of the unique interactions of CXCL8 isoforms with their receptors, we cannot assume that the retrieval of tadpole and adult frog skin granulocytes using rCXCL8a and rCXCL8b, as described here, does not yield multiple skin granulocyte populations. Ultimately, it will be of great benefit to disentangle the unique interactions of CXCL8 isoforms with their receptors.

Despite the differences between mammalian mast cells and the *X. laevis* esterase-positive skin granulocytes described here, the two cell types share in common their robust expression of antiviral interferon cytokines (Lopušná et al. 2013). It is somewhat intuitive that resident skin immune cells of animals that are constantly bombarded by viral pathogens through their environments, would possess the capacity to orchestrate antiviral immune responses. When considered in the context of our recent work demonstrating the robust type I and type III interferon responses to skin FV3 infections of tadpole and adult *X. laevis* (Wendel et al. 2017, 2018), it is interesting that the resident skin granulocytes possessed relatively robust expression of both type I and III IFN genes while pharmacological depletion of these cells rendered tadpoles more susceptible to FV3. In line with these findings, the tadpole skin granulocytes significantly upregulated the majority of these *ifn* transcripts upon challenge with FV3. Likewise, mammalian mast cells have been implicated in antiviral immunity (Fukuda et al. 2013) and have been shown to produce antiviral IFNs following stimulation (Kulka et al. 2004; Dietrich et al. 2010). However, it is noteworthy that the repertoires of *ifn* genes expressed by the tadpole and adult frog skin granulocytes do not entirely match the distinct whole skin *ifn* gene expression patterns seen between tadpole and adult *X. laevis* (Wendel et al. 2017). Such a discrepancy indicates that these resident skin granulocytes are not the sole source(s) of tadpole and adult frog skin *ifn* gene expression. It will be invaluable to learn through future studies the respective contribution of these skin granulocytes to amphibian antiviral IFN responses to FV3 and other relevant viruses.

Mast cells were first discovered in an amphibian species (Ehrlich 1877; Dines and Powell 1997) and perhaps not coincidentally, we report on the discovery of amphibian resident skin granulocyte population(s) exhibiting similarities to, as well as differences from mammalian mast cells. In turn, it is intriguing to consider just how unique the physiologies and habitats of amphibians are, as compared to those of more recently diverged terrestrial vertebrates against which we attempt to compare amphibian immune systems. As we face amphibian mass extinctions and concerning global declines (Wake and Vredenburg 2008), it is essential to develop a comprehensive understanding of the immune cells and components that define amphibians in the context of their distinctive ecophysiologies and pathogenic pressures.

Acknowledgements

KH and AY thank the GWU, Department of Biological Sciences for GTA support and support from the GWU Harlan Research program. DK thanks the Harlan Undergraduate Research Program. PR and AB thank the Thomas Jefferson High School internship program. LG thanks the GWU Department of Biology. This work was supported by a National Science Foundation CAREER Award (IOS: 1749427) to LG. The authors thank the two anonymous reviewers whose comments and suggestions helped to improve the content of this manuscript.

Author contributions

KH, MP, and LG conceived and designed the study. KH, MP, AY, DVK, PR, AB, and RW performed the experiments/collected the data. KH, MP, AY, RW, MJF, and LG analyzed and interpreted the data. LG contributed resources. KH, MP, MJF, and LG drafted or revised the manuscript.

Competing interests

The authors have declared that no competing interests exist.

Data availability statement

All relevant data are within the paper and Supplementary Material.

Supplementary material

The following Supplementary Material is available with the article through the journal website at doi:10.1139/facets-2020-0010.

Supplementary Material 1

References

Abonia JP, Austen KF, Rollins BJ, Joshi SK, Flavell RA, Kuziel WA, et al. 2005. Constitutive homing of mast cell progenitors to the intestine depends on autologous expression of the chemokine receptor CXCR2. Blood, 105(11): 4308–4313. PMID: 15705791 DOI: 10.1182/blood-2004-09-3578

Baccari GC, Pinelli C, Santillo A, Minucci S, and Rastogi RK. 2011. Mast cells in nonmammalian vertebrates: an overview. International Review of Cell and Molecular Biology, 290: 1–53. PMID: 21875561 DOI: 10.1016/B978-0-12-386037-8.00006-5

Berger L, Speare R, Daszak P, Green DE, Cunningham AA, Goggin CL, et al. 1998. Chytridiomycosis causes amphibian mortality associated with population declines in the rain forests of Australia and Central America. Proceedings of the National Academy of Sciences of the United States of America, 95(15): 9031–9036. PMID: 9671799 DOI: 10.1073/pnas.95.15.9031

Braun MG, Csernok E, Rogener-Schwarz W, Ludwig WD, Muller-Hermelink HK, Gross WL, et al. 1996. Monoclonal antibody WGM1 directed against proteinase 3: an immunohistochemical marker for naphthol ASD chloroacetate. Hematological Oncology, 14(2): 83–90. PMID: 8876637 DOI: 10.1002/(SICI)1099-1069(199606)14:2<83::AID-HON570>3.0.CO;2-N

Brunner JL, and Yarber CM. 2018. Evaluating the importance of environmental persistence for ranavirus transmission and epidemiology. Advances in Virus Research, 101: 129–148. PMID: 29908588 DOI: 10.1016/bs.aivir.2018.02.005

Cai Z, Gao C, Zhang Y, and Xing K. 2009. Functional characterization of the ELR motif in piscine ELR CXC-like chemokine. Marine Biotechnology, 11(4): 505–512. PMID: 19048342 DOI: 10.1007/s10126-008-9165-y

Carey C, Cohen N, and Rollins-Smith L. 1999. Amphibian declines: an immunological perspective. Developmental & Comparative Immunology, 23(6): 459–472. PMID: 10512457 DOI: 10.1016/S0145-305X(99)00028-2

Carrillo-Farga J, Castell A, Pérez A, and Rondán A. 1990. Langerhans-like cells in amphibian epidermis. Journal of Anatomy, 172: 39–45. PMID: 2148747

Castell-Rodríguez AE, Sampedro-Carrillo EA, Herrera-Enriquez MA, and Rondán-Zárate A. 2001. Non-specific esterase-positive dendritic cells in epithelia of the frog *Rana pipiens*. The Histochemical Journal, 33(5): 311–316. PMID: 11563545 DOI: 10.1023/A:1017985209296

Clark-Lewis I, Schumacher C, Baggiolini M, and Moser B. 1991. Structure-activity relationships of interleukin-8 determined using chemically synthesized analogs. Critical role of NH2-terminal residues and evidence for uncoupling of neutrophil chemotaxis, exocytosis, and receptor binding activities. The Journal of Biological Chemistry, 266(34): 23128–23134. PMID: 1744111

Clark-Lewis I, Dewald B, Geiser T, Moser B, and Baggiolini M. 1993. Platelet factor 4 binds to interleukin 8 receptors and activates neutrophils when its N terminus is modified with Glu-Leu-Arg. Proceedings of the National Academy of Sciences of the United States of America, 90(8): 3574–3577. PMID: 8475106 DOI: 10.1073/pnas.90.8.3574

Colombo BM, Scalvenzi T, Benlamara S, and Pollet N. 2015. Microbiota and mucosal immunity in amphibians. Frontiers in Immunology, 6: 111. PMID: 25821449 DOI: 10.3389/fimmu.2015.00111

Dietrich N, Rohde M, Geffers R, Kröger A, Hauser H, Weiss S, et al. 2010. Mast cells elicit proinflammatory but not type I interferon responses upon activation of TLRs by bacteria. Proceedings of the National Academy of Sciences of the United States of America, 107(19): 8748–8753. PMID: 20421474 DOI: 10.1073/pnas.0912551107

Dines KC, and Powell HC. 1997. Mast cells interactions with the nervous system: relationship to mechanisms of disease. Journal of Neuropathology and Experimental Neurology, 56(6): 627–640. PMID: 9184654 DOI: 10.1097/00005072-199706000-00001

Dobson JT, Seibert J, Teh EM, Da'as S, Fraser RB, Paw BH, et al. 2008. Carboxypeptidase A5 identifies a novel mast cell lineage in the zebrafish providing new insight into mast cell fate determination. Blood, 112(7): 2969–2972. PMID: 18635811 DOI: 10.1182/blood-2008-03-145011

Duffus ALJ, and Cunningham AA. 2010. Major disease threats to European amphibians. Herpetological Journal, 20(3): 117–127.

Ehrlich P. 1877. Beiträge zur Kenntniss der Anilinfärbungen und ihrer Verwendung in der mikroskopischen Technik. Archiv für mikroskopische Anatomie, 13(1): 263–277. DOI: 10.1007/BF02933937

Feder ME, and Burggren WW. 1992. Environmental physiology of the amphibians. University of Chicago Press, Chicago, Illinois.

Flechas SV, Acosta-Gonzalez A, Escobar LA, Kueneman JG, Sanchez-Quitian ZA, Parra-Giraldo CM, et al. 2019. Microbiota and skin defense peptides may facilitate coexistence of two sympatric Andean frog species with a lethal pathogen. The ISME Journal, 13(2): 361–373. PMID: 30254321 DOI: 10.1038/s41396-018-0284-9

Fukuda M, Ushio H, Kawasaki J, Niyonsaba F, Takeuchi M, Baba T, et al. 2013. Expression and functional characterization of retinoic acid-inducible gene-I-like receptors of mast cells in response to viral infection. Journal of Innate Immunity, 5(2): 163–173. PMID: 23171655 DOI: 10.1159/000343895

Galli SJ, and Wershil BK. 1996. The two faces of the mast cell. Nature, 381(6577): 21–22. PMID: 8609979 DOI: 10.1038/381021a0

Green DE, Converse KA, and Schrader AK. 2002. Epizootiology of sixty-four amphibian morbidity and mortality events in the USA, 1996–2001. Annals of the New York Academy of Sciences, 969: 323–339. PMID: 12381613 DOI: 10.1111/j.1749-6632.2002.tb04400.x

Grogan LF, Robert J, Berger L, Skerratt LF, Scheele BC, Castley JG, et al. 2018. Review of the amphibian immune response to chytridiomycosis, and future directions. Frontiers in Immunology, 9: 2536. PMID: 30473694 DOI: 10.3389/fimmu.2018.02536

Gurish MF, Tao H, Abonia JP, Arya A, Friend DS, Parker CM, et al. 2001. Intestinal mast cell progenitors require CD49dβ7 (α4β7 integrin) for tissue-specific homing. The Journal of Experimental Medicine, 194(9): 1243–1252. PMID: 11696590 DOI: 10.1084/jem.194.9.1243

Halliday TR. 2008. Why amphibians are important. International Zoo Yearbook, 42(1): 7–14. DOI: 10.1111/j.1748-1090.2007.00037.x

Hayes TB, Falso P, Gallipeau S, and Stice M. 2010. The cause of global amphibian declines: a developmental endocrinologist's perspective. Journal of Experimental Biology, 213(6): 921–933. PMID: 20190117 DOI: 10.1242/jeb.040865

Ingaleshwar PS, Pandit S, Desai D, Redder CP, Shetty AS, and Mithun KM. 2016. Immunohistochemical analysis of angiogenesis by CD34 and mast cells by toluidine blue in different grades of oral squamous cell carcinoma. Journal of Oral and Maxillofacial Pathology, 20(3): 467–473. PMID: 27721613 DOI: 10.4103/0973-029X.190950

Johnson AR, and Moran NC. 1974. Interaction of toluidine blue and rat mast cells: histamine release and uptake and release of the dye. Journal of Pharmacology and Experimental Therapeutics, 189(1): 221–234. PMID: 4132668

Koubourli DV, Wendel ES, Yaparla A, Ghaul JR, and Grayfer L. 2017. Immune roles of amphibian (*Xenopus laevis*) tadpole granulocytes during Frog Virus 3 ranavirus infections. Developmental & Comparative Immunology, 72: 112–118. PMID: 28238879 DOI: 10.1016/j.dci.2017.02.016

Koubourli DV, Yaparla A, Popovic M, and Grayfer L. 2018. Amphibian (*Xenopus laevis*) interleukin-8 (CXCL8): a perspective on the evolutionary divergence of granulocyte chemotaxis. Frontiers in Immunology, 9: 2058. PMID: 30258441 DOI: 10.3389/fimmu.2018.02058

Kulka M, Alexopoulou L, Flavell RA, and Metcalfe DD. 2004. Activation of mast cells by double-stranded RNA: evidence for activation through Toll-like receptor 3. Journal of Allergy and Clinical Immunology, 114(1): 174–182. PMID: 15241362 DOI: 10.1016/j.jaci.2004.03.049

Kurane I, Hebblewaite D, Brandt WE, and Ennis FA. 1984. Lysis of dengue virus-infected cells by natural cell-mediated cytotoxicity and antibody-dependent cell-mediated cytotoxicity. Journal of Virology, 52(1): 223–230. PMID: 6207308 DOI: 10.1128/JVI.52.1.223-230.1984

Lopušná K, Režuchová I, Betáková T, Škorvanová L, Tomášková J, Lukáčiková L, et al. 2013. Interferons lambda, new cytokines with antiviral activity. Acta Virologica, 57(2): 171–179. PMID: 23600875 DOI: 10.4149/av_2013_02_171

Mescher AL, Wolf WL, Moseman EA, Hartman B, Harrison C, Nguyen E, et al. 2007. Cells of cutaneous immunity in *Xenopus*: studies during larval development and limb regeneration. Developmental & Comparative Immunology, 31(4): 383–393. PMID: 16926047 DOI: 10.1016/j.dci.2006.07.001

Metcalfe DD, Baram D, and Mekori YA. 1997. Mast cells. Physiological Reviews, 77(4): 1033–1079. PMID: 9354811 DOI: 10.1152/physrev.1997.77.4.1033

Minnicozzi M, Sawyer RT, and Fenton MJ. 2011. Innate immunity in allergic disease. Immunological Reviews, 242(1): 106–127. PMID: 21682741 DOI: 10.1111/j.1600-065X.2011.01025.x

Morales HD, Abramowitz L, Gertz J, Sowa J, Vogel A, and Robert J. 2010. Innate immune responses and permissiveness to ranavirus infection of peritoneal leukocytes in the frog *Xenopus laevis*. Journal of Virology, 84(10): 4912–4922. PMID: 20200236 DOI: 10.1128/JVI.02486-09

Nieto-Patlán A, Campillo-Navarro M, Rodríguez-Cortés O, Muñoz-Cruz S, Wong-Baeza I, Estrada-Parra S, et al. 2015. Recognition of *Candida albicans* by Dectin-1 induces mast cell activation. Immunobiology, 220(9): 1093–1100. PMID: 26001731 DOI: 10.1016/j.imbio.2015.05.005

Nieuwkoop PD, and Faber J (*Editors*). 1975. Normal table of Xenopus laevis (Daudin). North-Holland Publishing Co., Amsterdam, the Netherlands.

Papadopoulos EJ, Fitzhugh DJ, Tkaczyk C, Gilfillan AM, Sassetti C, Metcalfe DD, et al. 2000. Mast cells migrate, but do not degranulate, in response to fractalkine, a membrane-bound chemokine expressed constitutively in diverse cells of the skin. European Journal of Immunology, 30(8): 2355–2361. PMID: 10940926 DOI: 10.1002/1521-4141(2000)30:8<2355::AID-IMMU2355>3.0.CO;2-#

Pawlick RL, Wink J, Pepper AR, Bruni A, Abualhassen N, Rafiei Y, et al. 2016. Reparixin, a CXCR1/2 inhibitor in islet allotransplantation. Islets, 8(5): 115–124. PMID: 27328412 DOI: 10.1080/19382014.2016.1199303

Pelli AA, Azevedo RA, Cinelli LP, Mourao PA, and de Brito-Gitirana L. 2007. Dermatan sulfate is the major metachromatic glycosaminoglycan in the integument of the anuran *Bufo ictericus*. Comparative Biochemistry and Physiology Part B: Biochemistry and Molecular Biology, 146(2): 160–165. PMID: 17137817 DOI: 10.1016/j.cbpb.2006.10.098

Piliponsky AM, Acharya M, and Shubin NJ. 2019. Mast cells in viral, bacterial, and fungal infection immunity. International Journal of Molecular Sciences, 20(12): 2851. PMID: 31212724 DOI: 10.3390/ijms20122851

Puebla-Osorio N, Sarchio SNE, Ullrich SE, and Byrne SN. 2017. Detection of infiltrating mast cells using a modified toluidine blue staining. Methods in Molecular Biology, 1627: 213–222. PMID: 28836204 DOI: 10.1007/978-1-4939-7113-8_14

Qi X, Hong J, Chaves L, Zhuang Y, Chen Y, Wang D, et al. 2013. Antagonistic regulation by the transcription factors C/EBPα and MITF specifies basophil and mast cell fates. Immunity, 39(1): 97–110. PMID: 23871207 DOI: 10.1016/j.immuni.2013.06.012

Rachowicz LJ, and Vredenburg VT. 2004. Transmission of *Batrachochytrium dendrobatidis* within and between amphibian life stages. Diseases of Aquatic Organisms, 61(1–2): 75–83. PMID: 15584413 DOI: 10.3354/dao061075

Rigby KM, and DeLeo FR. 2012. Neutrophils in innate host defense against *Staphylococcus aureus* infections. Seminars in Immunopathology, 34(2): 237–259. PMID: 22080185 DOI: 10.1007/s00281-011-0295-3

Rikitake Y, and Takai Y. 2011. Directional cell migration: regulation by small G proteins, nectin-like molecule-5, and afadin. International Review of Cell and Molecular Biology, 287: 97–143. PMID: 21414587 DOI: 10.1016/B978-0-12-386043-9.00003-7

Sang Y, Liu Q, Lee J, Ma W, McVey DS, and Blecha F. 2016. Expansion of amphibian intronless interferons revises the paradigm for interferon evolution and functional diversity. Scientific Reports, 6: 29072. PMID: 27356970 DOI: 10.1038/srep29072

Scheele BC, Pasmans F, Skerratt LF, Berger L, Martel A, Beukema W, et al. 2019. Amphibian fungal panzootic causes catastrophic and ongoing loss of biodiversity. Science, 363(6434): 1459–1463. PMID: 30923224 DOI: 10.1126/science.aav0379

Schueller E, Peutsch M, Bohacek LG, and Gupta RK. 1967. A simplified toluidine blue stain for mast cells. Canadian Journal of Medical Technology, 29(4): 137–138. PMID: 4169058

Skerratt LF, Berger L, Speare R, Cashins S, McDonald KR, Phillott AD, et al. 2007. Spread of chytridiomycosis has caused the rapid global decline and extinction of frogs. EcoHealth, 4(2): 125. DOI: 10.1007/s10393-007-0093-5

Sridharan G, and Shankar AA. 2012. Toluidine blue: a review of its chemistry and clinical utility. Journal of Oral and Maxillofacial Pathology, 16(2): 251–255. PMID: 22923899 DOI: 10.4103/0973-029X.99081

Stuart SN, Chanson JS, Cox NA, Young BE, Rodrigues AS, Fischman DL, et al. 2004. Status and trends of amphibian declines and extinctions worldwide. Science, 306(5702): 1783–1786. PMID: 15486254 DOI: 10.1126/science.1103538

Tas J. 1977. Microspectrophotometric detection of heparin in young and adult rat mast cells, human mast cells and human basophilic granulocytes stained metachromatically with toluidine blue O. Acta Histochemica. Supplementband, 18: 95–100. PMID: 95796

Ulich TR, Del Castillo J, McNiece IK, Yi ES, Alzona CP, Yin SM, et al. 1991. Stem cell factor in combination with granulocyte colony-stimulating factor (CSF) or granulocyte-macrophage CSF synergistically increases granulopoiesis in vivo. Blood, 78(8): 1954–1962. PMID: 1717076 DOI: 10.1182/blood.V78.8.1954.1954

Varricchi G, Raap U, Rivellese F, Marone G, and Gibbs BF. 2018. Human mast cells and basophils-How are they similar how are they different? Immunological Reviews, 282(1): 8–34. PMID: 29431214 DOI: 10.1111/imr.12627

Wake DB, and Vredenburg VT. 2008. Colloquium paper: are we in the midst of the sixth mass extinction? A view from the world of amphibians. Proceedings of the National Academy of Sciences of the United States of America, 105(Suppl. 1): 11466–11473. PMID: 18695221 DOI: 10.1073/pnas.0801921105

Wang T, and Secombes CJ. 2015. The evolution of IL-4 and IL-13 and their receptor subunits. Cytokine, 75(1): 8–13. PMID: 26005057 DOI: 10.1016/j.cyto.2015.04.012

Wendel ES, Yaparla A, Koubourli DV, and Grayfer L. 2017. Amphibian (*Xenopus laevis*) tadpoles and adult frogs mount distinct interferon responses to the Frog Virus 3 ranavirus. Virology, 503: 12–20. PMID: 28081430 DOI: 10.1016/j.virol.2017.01.001

Wendel ES, Yaparla A, Melnyk MLS, Koubourli DV, and Grayfer L. 2018. Amphibian (*Xenopus laevis*) tadpoles and adult frogs differ in their use of expanded repertoires of type I and type III interferon cytokines. Viruses, 10(7): 372. PMID: 30018186 DOI: 10.3390/v10070372

Yang FC, Tsuji K, Oda A, Ebihara Y, Xu MJ, Kaneko A, et al. 1999. Differential effects of human granulocyte colony-stimulating factor (hG-CSF) and thrombopoietin on megakaryopoiesis and platelet function in hG-CSF receptor-transgenic mice. Blood, 94(3): 950–958. PMID: 10419886 DOI: 10.1182/blood.V94.3.950.415a18_950_958

Yaparla A, Wendel ES, and Grayfer L. 2016. The unique myelopoiesis strategy of the amphibian *Xenopus laevis*. Developmental & Comparative Immunology, 63: 136–143. PMID: 27234705 DOI: 10.1016/j.dci.2016.05.014

Yaparla A, Popovic M, and Grayfer L. 2018. Differentiation-dependent antiviral capacities of amphibian (*Xenopus laevis*) macrophages. The Journal of Biological Chemistry, 293(5): 1736–1744. PMID: 29259133 DOI: 10.1074/jbc.M117.794065